Review:

A 20-Year Bibliometric and VOSviewer-Based Analysis (2006–2025) on Functionalized Carbon Adsorbents for Methylene Blue Removal

Maria Ulfa[1*], Rizka Fauzia Hanif[1], Cindy Nur Anggreani[1], and Ayu Tri Rahmawati[2]

[1]*Chemistry Education Study Program, Faculty of Teacher Training and Education, Sebelas Maret University, Jl. Ir. Sutami 36A, Surakarta 57126, Indonesia*

[2]*Magister of Chemistry Education Study Program, Faculty of Teacher Training and Education, Sebelas Maret University, Jl. Ir. Sutami 36A, Surakarta 57126, Indonesia*

* ***Corresponding author:***

tel: +62-81392932270
email: mariaulfa@staff.uns.ac.id

Received: July 31, 2025
Accepted: January 20, 2026

DOI: 10.22146/ijc.109906

Abstract: *The increasing discharge of synthetic dyes, particularly methylene blue (MB), from textile effluents poses significant environmental and health challenges, necessitating effective remediation strategies. Among various approaches, adsorption has emerged as a promising technique due to its operational simplicity, cost-effectiveness, and high efficiency. This review focuses on the surface chemistry and adsorption behavior of MB on functionalized carbon-based materials. Emphasis is placed on the physicochemical properties, surface modifications, and functional groups that govern adsorption capacity and selectivity. Recent advancements in the synthesis of engineered carbonaceous adsorbents—such as activated carbon, graphene derivatives, carbon nanotubes, and novel carbon composites—are critically examined in relation to their structural characteristics and interaction mechanisms with MB molecules. Special attention is given to the ACHC-KOM-1 carbon composite, which demonstrates remarkable photocatalytic-assisted adsorption, achieving complete (100%) degradation of MB under optimized conditions. By elucidating the key parameters that influence adsorption performance, this study provides valuable insights into the rational design of high-efficiency adsorbents for sustainable wastewater treatment applications.*

Keywords: *adsorption; functionalized carbon; methylene blue; adsorption parameters; bibliometric analysis*

■ INTRODUCTION

Industrial effluents are among the major contributors to global water pollution, particularly through the release of synthetic dyes such as methylene blue (MB), methyl orange (MO), and rhodamine red (RR). MB is a cationic thiazine dye widely used in textile dyeing, paper printing, leather processing, and medical diagnostics [1-2]. Its aromatic heterocyclic structure, high chemical stability, and resistance to biodegradation contribute to its persistence in aquatic environments and make it difficult to remove using conventional treatment methods [2]. These dyes are persistent, toxic, and resistant to conventional wastewater treatment methods, posing serious environmental and health hazards.

Conventional approaches for MB removal, including coagulation–flocculation, membrane filtration, and advanced oxidation processes (AOPs), have been widely applied; however, these methods frequently suffer from incomplete dye removal, high operational and maintenance costs, excessive sludge generation, membrane fouling, and the risk of secondary pollution due to chemical additives or partial oxidation by-products. In contrast, adsorption-based techniques—particularly those employing carbon-based materials [1]—offer higher removal efficiency, operational simplicity, reusability, and minimal secondary pollution, making them more attractive for sustainable wastewater treatment [2].

With increasing demand for clean water and sustainable environmental solutions, research attention has turned to the development of efficient, eco-friendly adsorbents capable of removing these pollutants. Among these, carbon-based materials have gained prominence due to their high surface area, tunable porosity, surface functionality, and potential for modification to enhance adsorption and regeneration performance [3-5].

Functionalized carbon adsorbents—encompassing activated carbon [6], biochar [7], carbon nanotubes [8], and graphene-based composites [9]—represent a crucial class of materials with wide applicability in wastewater treatment [10-12]. The addition of heteroatoms or metal oxides such as TiO_2, ZnO, and Fe_3O_4 to the carbon matrix has been shown to enhance adsorption capacity, photocatalytic activity, and recyclability [13-15]. In recent years, a new research trend has emerged focusing on hybrid systems that combine adsorption and photocatalysis, integrating materials such as metal–organic frameworks (MOFs), hydrogels, and magnetic composites to improve pollutant degradation efficiency and material recovery [16-17].

Given the rapid growth of publications in this field, a comprehensive bibliometric analysis is essential to map the scientific evolution, collaboration networks, and thematic developments over the past two decades. Bibliometric mapping enables the identification of core research areas, influential authors, and emerging topics, providing a data-driven overview of how the field has evolved. This study applies such an approach to explore the global research landscape on functionalized carbon adsorbents for MB removal between 2006 and 2025, offering a systematic view of trends, hotspots, and collaborative patterns using Scopus data analyzed with VOSviewer.

■ METHODOLOGY

This study employed a bibliometric approach to analyze research trends, thematic evolution, and collaborative networks related to functionalized carbon adsorbents for MB removal over the past two decades (2006–2026). The bibliometric data were obtained from the Scopus database, widely recognized for comprehensive, high-quality coverage of the scientific literature. The search was conducted using the following keywords: adsorption, functionalized carbon, MB, adsorption parameters, and regeneration. The search was limited to journal articles only to ensure the inclusion of peer-reviewed scientific works.

The publication year range was set from 2006 to 2026. However, since no publications were indexed for 2026 at the time of data collection, the effective coverage period was 2006–2025. The retrieved data were exported in CSV format for compatibility with VOSviewer software. The dataset contained a total of 15,586 documents distributed as follows: 6,218 documents from 2006 to 2020; 3,618 documents from 2021 to 2023; 5,598 documents in 2024; 152 documents in 2025; and none in 2026.

Bibliometric mapping and visualization were performed using VOSviewer (version 1.6.20), a specialized software for constructing and visualizing bibliometric networks. Three visualization modes were applied: Network visualization to show co-occurrence relationships among keywords, overlay visualization to display the temporal evolution of keywords by publication year, and density visualization to illustrate areas of high research concentration and thematic intensity.

For keyword analysis, a co-occurrence network was constructed with a minimum threshold of five occurrences. Co-authorship networks were analyzed at three hierarchical levels: country level (threshold 10), institution level (threshold 10), and author level (threshold 10). The resulting visual maps provided insights into the main research themes, influential contributors, and the evolution of functionalized carbon-based adsorption studies over the last 19 years. These visualizations were interpreted to identify dominant research clusters, emerging topics, and collaborative patterns within the field.

■ RESULTS AND DISCUSSION

The bibliometric trend shows a steady increase in publications on carbon-based adsorbents for dye removal, particularly after 2010. A significant rise was

observed from 2019 to 2024, indicating growing global attention toward sustainable adsorption technologies. Early studies (2006–2015) primarily focused on the fundamental mechanisms of adsorption, equilibrium modeling, and kinetics. In contrast, publications from 2016 onward emphasized material modification, functionalization, and regeneration, reflecting a shift toward performance enhancement and reusability (Fig. 1).

The VOSviewer overlay visualization revealed that the terms "adsorption", "activated carbon", and "methylene blue" dominate the research network, indicating their central role in this domain. In earlier years, the focus was on conventional adsorbents and basic characterization. However, in the most recent decade, new terms such as "graphene oxide", "titanium dioxide", "composites", "visible light", and "photocatalysis" have appeared more frequently, suggesting a transition toward multifunctional hybrid materials capable of both adsorption and photocatalytic degradation. Additionally, keywords such as "regeneration", "reusability", "hydrogel", and "biochar" exhibit increasing co-occurrence, highlighting the recent emphasis on sustainable and circular design principles in material synthesis. The density visualization further confirms that current research hotspots are concentrated around "graphene oxide composites" and "TiO_2". The VOSviewer overlay visualization revealed that the terms "adsorption", "activated carbon", and "methylene blue" dominate the research network, indicating their central role in this domain. In earlier years, the focus was on conventional adsorbents and basic characterization. However, in the most recent decade, new terms such as "graphene oxide", "titanium dioxide", "composites", "visible light", and "photocatalysis" have appeared more frequently, suggesting a transition toward multifunctional hybrid materials capable of both adsorption and photocatalytic degradation. Additionally, keywords such as "regeneration", "reusability", "hydrogel", and "biochar" exhibit increasing co-occurrence, highlighting the recent emphasis on sustainable and circular design principles in material synthesis. The density visualization further confirms that current research hotspots are concentrated around "graphene oxide composites", "TiO_2–carbon hybrids", and "photodegradation under visible light", reflecting an interdisciplinary integration between adsorption science and advanced photocatalysis. The overlay visualization map (Fig. 2) highlights the temporal evolution of research keywords,

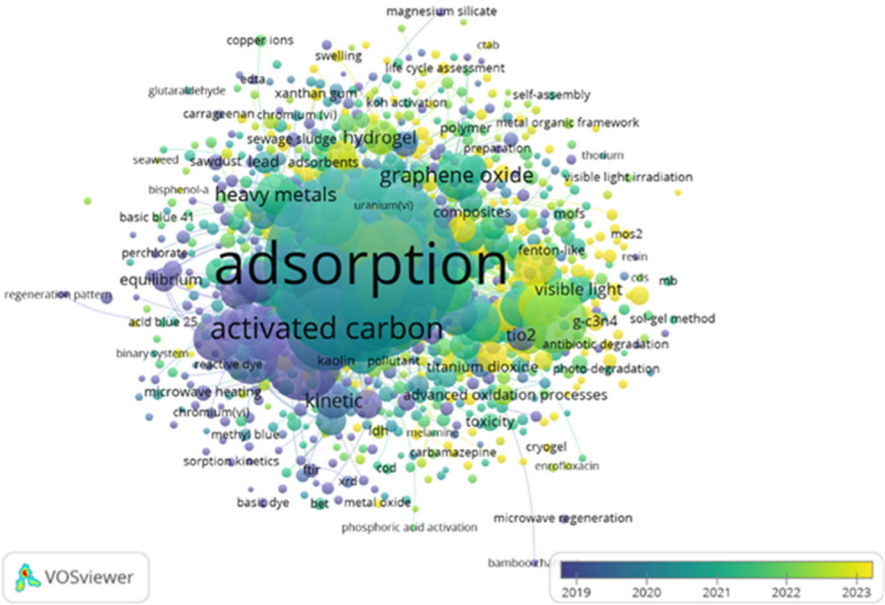

Fig 1. Overlay visualization map of keyword co-occurrence network for functionalized carbon adsorbents related to MB removal (Scopus database, 2006–2025)

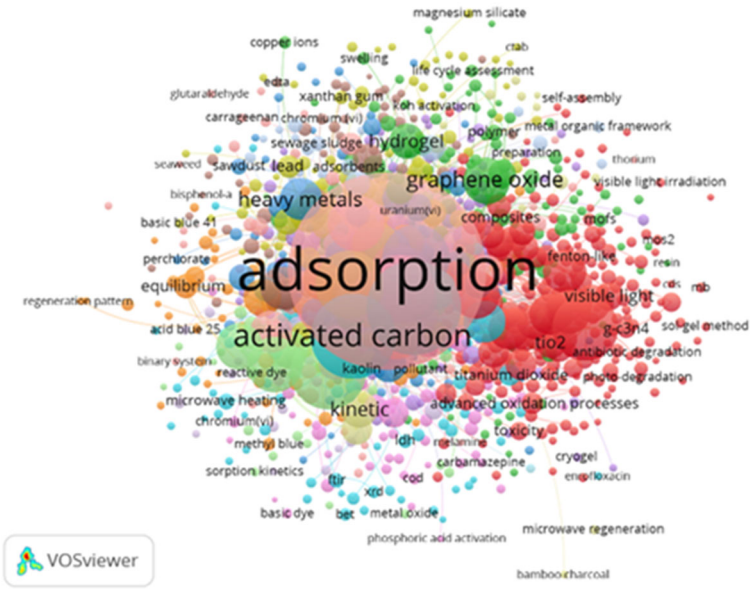

Fig 2. VOSviewer network visualization of keyword co-occurrence clusters for functionalized carbon adsorbents related to MB removal (Scopus data, 2006–2025; threshold = 5)

indicating a gradual shift from fundamental adsorption studies toward regeneration and functionalization of carbon-based adsorbents. Further analysis of co-authorship networks at the country and author levels is presented in the following sections to explore global collaboration patterns and research productivity.

Fig. 2 presents the VOSviewer network visualization of keyword co-occurrence related to functionalized carbon adsorbents for MB removal from 2006 to 2025. The map displays three dominant clusters representing the major research directions in this field. The red cluster focuses on the fundamentals of adsorption, including kinetics, isotherm models, and equilibrium studies, reflecting the core scientific basis of dye removal. The green cluster centers on activated carbon, graphene oxide, hydrogel, and composites, emphasizing material synthesis, surface modification, and structural optimization to enhance adsorption performance. Meanwhile, the blue cluster highlights visible light irradiation, TiO_2, and g-C_3N_4, representing the integration of adsorption with photocatalytic and hybrid systems for advanced pollutant degradation. Overall, "adsorption" and "activated carbon" emerge as the most prominent and interconnected terms, underscoring their pivotal role in carbon-based water purification research. The clustering pattern reveals an ongoing shift from conventional adsorption studies toward multifunctional carbon materials with improved surface activity, reusability, and environmental sustainability.

Fig. 3 illustrates the density visualization of keyword co-occurrence in adsorption-related studies. Brighter areas indicate high-frequency and strongly interconnected keywords, while darker areas represent less explored topics. The dominant terms—adsorption, activated carbon, graphene oxide, heavy metals, and TiO_2—highlight the central focus of research on carbon-based and metal oxide hybrid adsorbents. Emerging terms such as visible light, photodegradation, MOFs, and g-C_3N_4 suggest a growing trend toward multifunctional materials and integrated adsorption–photocatalysis systems. This density map provides an overview of the main thematic clusters and evolving research hotspots in adsorption studies over the past two decades.

The overlay visualization map of keyword co-occurrence from the Scopus database (2006–2025) with a threshold of 5 shows a highly dynamic and diversified landscape of adsorption research (Fig. 4). The largest and most dominant cluster is located in the center of the map, led by three closely interconnected core concepts: adsorption, activated carbon, and kinetic, indicating the

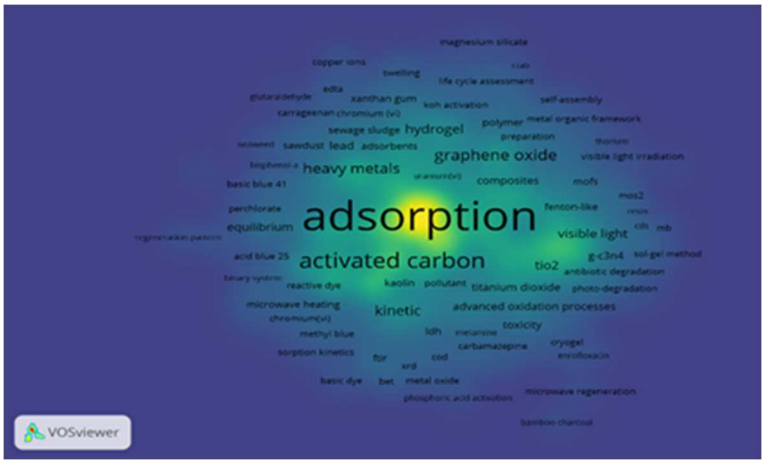

Fig 3. Density visualization map of keyword co-occurrence in adsorption research (Scopus data, 2006–2025; threshold = 5)

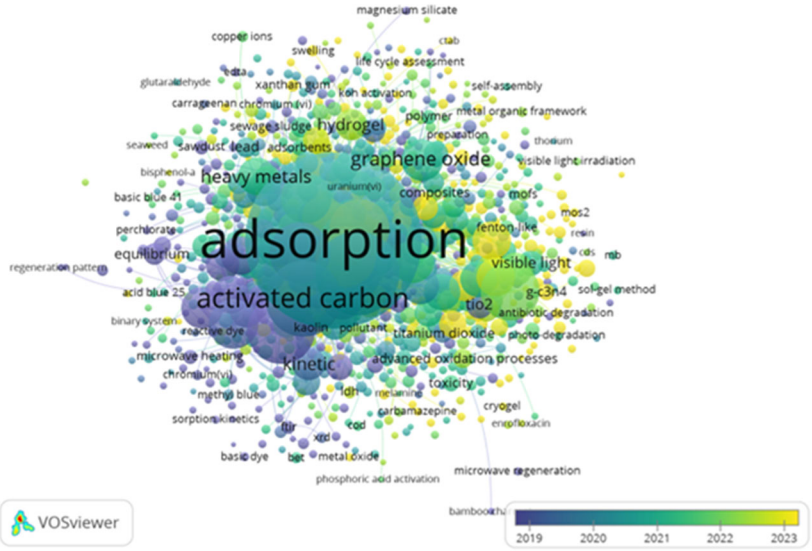

Fig 4. Overlay visualization map of keyword co-occurrence in adsorption research (Scopus data, 2006–2025; threshold = 5)

historical focus of research on adsorption using activated carbon with kinetic analysis. Around these core concepts, three main research zones can be identified based on the color gradient (2019–2023): (1) a more mature zone (dark blue, 2019–2020) covering topics such as heavy metals, graphene oxide, hydrogel, adsorbents, and KOH activation, indicating established research with extensive literature; (2) a transition zone (cyan-green, 2020–2021) covering polymers, composites, MOFs, and TiO_2, reflecting the evolution towards heterogeneous and multifunctional materials with photocatalytic activity; and (3) the emerging frontier zone (yellow-light green, 2022–2023) features the latest topics such as visible light irradiation, photo-degradation, antibiotic degradation, MOFs, sol-gel method, self-assembly, and life cycle assessment, which indicate a shift in research paradigms from passive adsorption to photocatalysis, sustainability considerations, and applications to pharmaceutical and biochemical contaminants. The peripheral position of topics such as magnesium silicate, CTAB, xanthan gum, and microwave heating indicates specific research or merging subfields that are still developing connections with the main themes. In contrast, the interconnection of heavy metals, sewage sludge, and basic blue 41 with the

core research reflects the practical relevance of adsorption in environmental remediation and industrial waste treatment.

Fig. 5 presents the global bibliometric landscape of research on functionalized carbon adsorbents for MB removal over the period 2006–2025, as visualized using VOSviewer. The figure integrates density visualization, overlay visualization, and network visualization to provide complementary insights into research productivity, temporal evolution, and international collaboration patterns. The density visualization highlights a strong concentration of research output in China and India, indicating their dominant roles in advancing studies on functionalized carbon materials for dye adsorption. The high-density regions associated with these countries reflect both extensive publication volume and their central influence on research themes such as carbon surface modification, pore structure engineering, and adsorption mechanisms. Additional contributions from Iran, South Korea, Pakistan, and Indonesia suggest a geographically expanding research landscape, particularly across Asia and the Middle East, while countries with lower density exhibit more limited or emerging engagement.

The overlay visualization illustrates the temporal progression of research activity. Early-stage studies, mainly appearing between 2006 and 2012 and represented by cooler color tones, focused on conventional activated carbon and fundamental adsorption behavior. In contrast, more recent publications (2020–2025), shown in

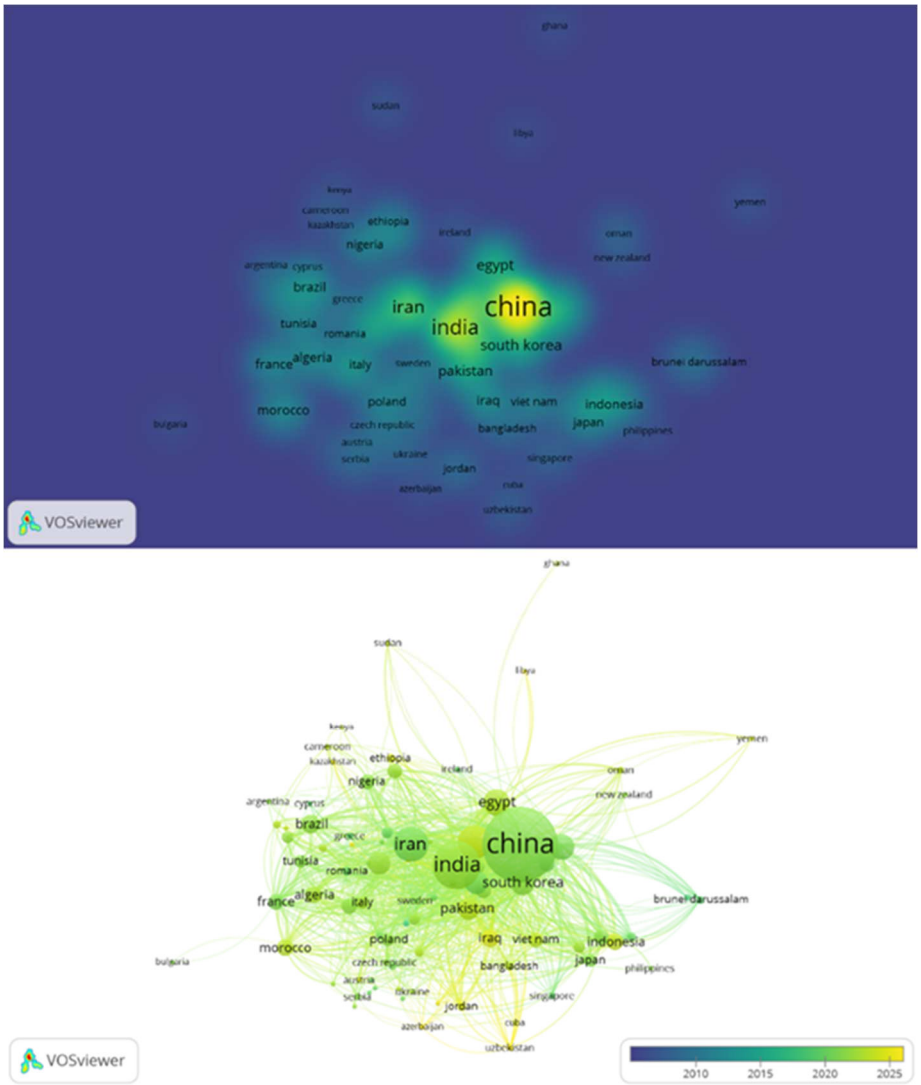

Fig 5. Global bibliometric mapping of research on functionalized carbon adsorbents for MB removal (2006–2025) based on VOSviewer analysis

warmer colors, demonstrate increased research intensity in countries such as China, India, Indonesia, Vietnam, and Bangladesh. This shift reflects a transition toward advanced research topics, including heteroatom-doped carbon, functionalized composites, and pore-size optimization aimed at enhancing MB adsorption efficiency. The persistent presence of China and India throughout the entire period further confirms their sustained leadership and long-term commitment to this research area. The network visualization reveals the structure and strength of international research collaborations. China, India, Iran, and South Korea appear as highly connected hubs, linking multiple regional clusters across Asia, Africa, and Europe. The dense interconnections among these countries indicate a collaborative, interdisciplinary research environment, driven by shared challenges in treating dye-contaminated wastewater. The observed clustering patterns suggest that while research activities are regionally concentrated, they remain globally integrated through extensive co-authorship networks. Overall, Fig. 5 demonstrates that research on functionalized carbon adsorbents for MB removal has experienced substantial growth and diversification over the past two decades. The increasing dominance of Asian countries, combined with expanding international collaboration, signifies a shift from conventional adsorption studies toward the rational design of high-surface-area, chemically functionalized carbon materials with tailored pore structures. These developments underscore the growing scientific maturity of the field and its relevance to sustainable and efficient wastewater treatment technologies. Fig. 6 extends the country-level patterns observed in Fig. 5 to the institutional scale, revealing a strong dominance of Asian universities and research institutions in studies on functionalized carbon adsorbents for MB removal. Universities and research centers from China, India, Iran, South Korea, and other Asian countries occupy the most central and highly connected positions in the network, indicating their substantial research output and extensive inter-institutional collaboration. In contrast, non-Asian institutions, primarily from Europe and other regions, appear as smaller or more peripheral nodes, reflecting comparatively lower publication intensity and a more specialized or complementary role. This institutional distribution directly mirrors the country-level dominance of Asia identified in Fig. 5, confirming that national research leadership is largely driven by the productivity and networking capacity of key universities.

Notably, Indonesian institutions are clearly represented in the mapping, including universities with strong chemistry and applied science faculties as well as national research bodies such as Badan Riset dan Inovasi Nasional (BRIN). Their presence, particularly in the more recent overlay visualization, indicates a growing

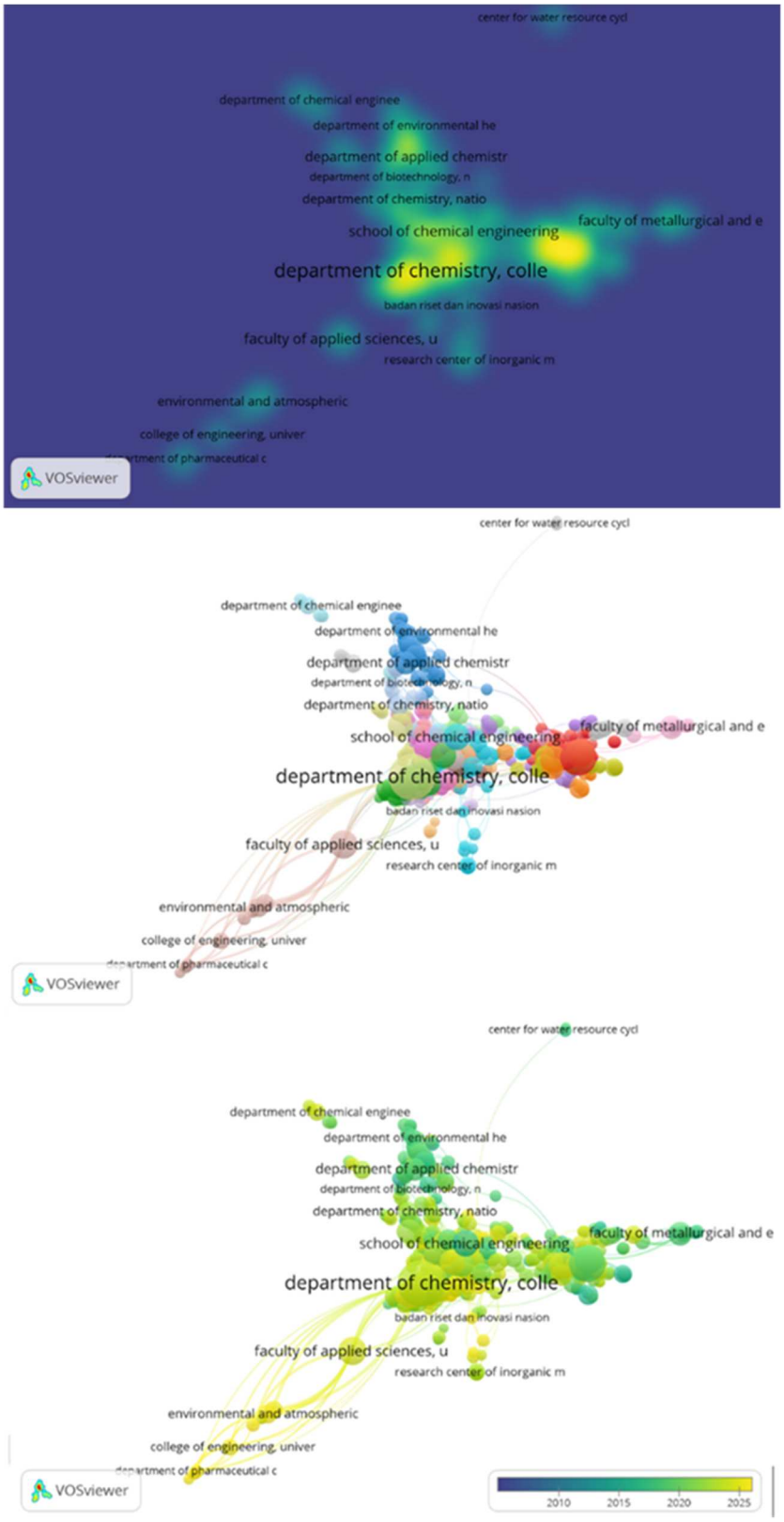

Fig 6. VOSviewer-based visualization of universities and research institutions in functionalized carbon adsorbent research for MB removal

institutional engagement aligned with national research priorities on environmental remediation and sustainable materials. From a policy perspective, this trend highlights the effectiveness of increased research funding, international collaboration schemes, and applied research incentives in Asia, while also suggesting opportunities for non-Asian universities to strengthen strategic partnerships. Overall, the transition from country-level dominance (Fig. 5) to institution-level leadership (Fig. 6) underscores the critical role of university-centered research ecosystems and sustained funding policies in advancing functionalized carbon adsorbents toward impactful wastewater treatment technologies.

Carbon as an Adsorbent for MB

Carbon-based adsorbents have attracted a lot of interest in analytical chemistry due to their many useful properties. These include high thermal stability, good extraction behavior, high adsorption capacity, and high selectivity. Graphene, carbon nanotubes, and various biopolymers, such as chitosan and biochar, are examples of adsorbents. Chemical precipitation, ion exchange, solvent extraction, nanofiltration, adsorption, and reverse osmosis are only a few of the extensively investigated and widely utilized wastewater treatment technologies. Adsorption is a significant technique among them because of its favorable characteristics, including high efficiency, low cost, and ease of operation. MB removal efficiency, however, is highly dependent on the type of carbon used. Carbon can be broken down into two categories, biomass-based and non-biomass-based carbons, depending on where it was produced.

Biomass-based carbon

Carbon obtained through pyrolysis of biomass is a natural resource that has been around for a long time. The physical and chemical properties of this carbon, as well as its wide range of potential uses across energy generation, agriculture, climate change mitigation, and environmental improvement, have garnered significant attention recently [13]. Biochar is made from biomass and contains carbon, which could improve soil fertility, agricultural land productivity, soil nutrient levels, water holding capacity, and greenhouse gas emission reduction [16]. Biomass carbon has many potential applications, including catalysis, supercapacitor production, gas system energy generation, gas adsorption, and contamination removal [17]. Carbon raw materials are often derived from organic waste such as agricultural residues, food waste, or biomass byproducts, thereby directly supporting waste reduction by transforming otherwise discarded materials into high-value functional adsorbents [18]. Biomass-based carbon generation is an attractive option for MB waste disposal because of its low cost and high efficiency [19-21]. Although pyrolysis is recognized as an energy-intensive process, its environmental impact can be mitigated through the utilization of biomass waste as feedstock, optimization of thermal efficiency, and consideration of the overall life cycle benefits [22-23]. By converting low-value organic residues into high-performance adsorbents, this approach supports waste valorization and aligns with green chemistry and circular economy principles. How much carbon is generated is determined by several variables, including the biomass used, the reaction medium, and the operating conditions. Carbon is created by slow pyrolysis and quick pyrolysis during the breakdown of biomass [24-26]. Important criteria that determine the carbon objective to be obtained are heating rate, pyrolysis temperature, and residence duration. The final carbon product has varying characteristics depending on the operational parameters [27-28]. Plant remnants, MSW, wood biomass, and animal dung are all listed in Table 1 as potential raw materials for trash. Sustainable resource management. Recent studies conducted during 2018-2022 reveal promising results when using natural carbon sources, including Areca catechu nut powder, polyurethane elastomer-sucrose, tannins, spent coffee grain, dried soybean dreg powder, eggshells, peanut shell (dry peanut shell), and corncob.

The data provided in Table 1 presents an insightful compilation of adsorption studies utilizing various biomass-derived and polymer-based precursors, emphasizing pyrolysis temperature, residence time, and material performance. The samples exhibit a broad spectrum of surface areas and pore volumes [29-30],

Table 1. Synthesis method of carbon and its physicochemical properties

Sample name	Pyrolysis (°C)	Time (h)	Precursor	Surface area (m^2/g)	Pore volume (cc/g)	q_{max} (mg/g)	Ref
Peat-derived AC	500	2	Peat	1100	-	382.00	[16]
Lignite-derived AC	750	1	Lignite	2400	-	279.00	[6]
Hard coal-derived AC	750	1	Hard coal	1014	0.210	200.00	[6]
Anthracite-derived AC	800	2	Anthracite	2514	-	385.00	[6]
Wood (*Acacia mangium*)-derived AC	600	2	Wood (*Acacia mangium*)	2300	-	15.00	[6]
Agricultural waste (Jatoba fruits)-derived AC	700	3	Agricultural waste (Jatoba fruits)	2000	-	400.00	[6]
Aquatic biomass (*Sargassum* macroalgae)-derived AC	600	2	Aquatic biomass (*Sargassum* macroalgae)	1700	-	43.00	[6]
Petroleum coke-derived AC	800	2	Petroleum coke	1800	-	194.00	[6]
Rice husks-derived AC	Low temp.	-	Rice husks (NaOH treatment-H_3PO_4 activation)	-	-	578.00	[6]
CF/ZIF-8 Composite	180	0.25	Agar powder, zinc nitrate hexahydrate, 2-methylimidazole	-	-	3132.00	[13]
Sucrose–graphene/chitosan carbon foams	900	1	Sucrose, graphene, chitosan	-	-	-	[17]
Sucrose-derived-bio-carbon foams	1200	-	-	-	-	-	[17]
Coal-based carbon foams	1100	-	Coal-based precursor	-	-	-	[17]
MOF/Carbon foam composite	800	-	-	-	-	1846.65	[17]
Magnetic nanoporous carbon (Fe_3O_4/NPC)	800	1	Dried soybean dreg powder	2611	2.210	2636.00	[18]
Peat-derived AC	850	1	Eggshells	324	-	299.40	[19]
Lignite-derived AC	800	2	Peanut shell (Dried peanut shell)	868	0.459	555.60	[20]
Hard Coal-derived AC	900	2	Corncob	1004	0.899	232.18	[3]
Anthracite-derived AC	1000	1	Orange peel				[21]
Wood (*Acacia mangium*)-derived AC	800	1	Pamelo peel				[22]
Agricultural waste (Jatoba fruits)-derived AC	850	1	Shaddoc peel				[23]
Aquatic biomass (*Sargassum* macroalgae)-derived AC	800	2	Banana Peel				[24]
Petroleum coke-derived AC	900	2	Waste orange				[25]
Rice husks derived AC	800	1	Cornstalk				[26]
CF/ZIF-8 Composite	850	1	Bagasse				[27]

highlighting the critical influence of precursor type [31-33] and pyrolysis conditions on adsorbent properties [34-37]. For instance, ANCs derived from *Areca catechu* nut powder achieved a remarkable surface area of 2132 m^2/g and a pore volume of 3.4 cc/g, corresponding to a maximum adsorption capacity (q_{max}) of 333.3 mg/g. Similarly, soybean dreg-derived SDB-6-K displayed an exceptionally high surface area of 2611 m^2/g and q_{max} of 2636 mg/g, underscoring its efficiency as an adsorbent for pollutant removal. A notable trend is observed in the EFAC1 series, where increasing pyrolysis time at 1000 °C resulted in significant improvements in adsorbent properties. For example, EFAC1 with a pyrolysis duration of 1.6 h demonstrated a surface area of 2172 m^2/g, a pore volume of 1.08 cc/g, and an outstanding q_{max} of 592 mg/g. This showcases the importance of fine-tuning pyrolysis parameters to optimize the material's textural properties and adsorption performance. Comparatively, precursors such as spent coffee grain (e.g., N-CGNM4) and peanut shell (PSAC) achieved moderate adsorption capacities, emphasizing the variability in precursor efficacy. The diverse range of precursors, from

agricultural residues (e.g., corncob and banana peel) to polymer-elastomer composites, reflects the ongoing exploration of sustainable adsorbents for environmental remediation [38-39]. The materials' performance metrics underscore their potential to address global challenges such as water purification and pollutant adsorption. By integrating green chemistry principles with advanced materials engineering, these studies pave the way for scalable, eco-friendly solutions, that align with circular economy goals and environmental sustainability.

Generally, pyrolysis, carbonization with inert gas, activation with CO_2, dry carbonization, and gasification of biomass, entanglement of $CaCl_2$ as an ammonia adsorbent, and MgO as a hard template are employed in the production of carbon from natural sources (Fig. 7). The usual pyrolysis process is conducted at 800–1000 °C for 0.5–2.0 h [40-43]. Even though some research has only used one variable to achieve maximum porosity, low temperature and rapid time remain the preferred method. For time efficiency, pyrolysis, or carbonization at 1000 °C under an inert gas stream for a short time is preferred over a lower temperature for a longer time [44-46]. However, the number of micropores will increase and be inaccessible to the adsorbate, as indicated by the comparatively low capacity compared to pyrolyzed carbon at 1000 °C for a longer period, allowing the conversion of all carbon precursors while permitting the production of high porosity [47-48].

Adding carbon surface components or functional groups derived from natural materials has led to the creation of several composites and modifications [49-52]. Carbon or carbon-modified composites have an average

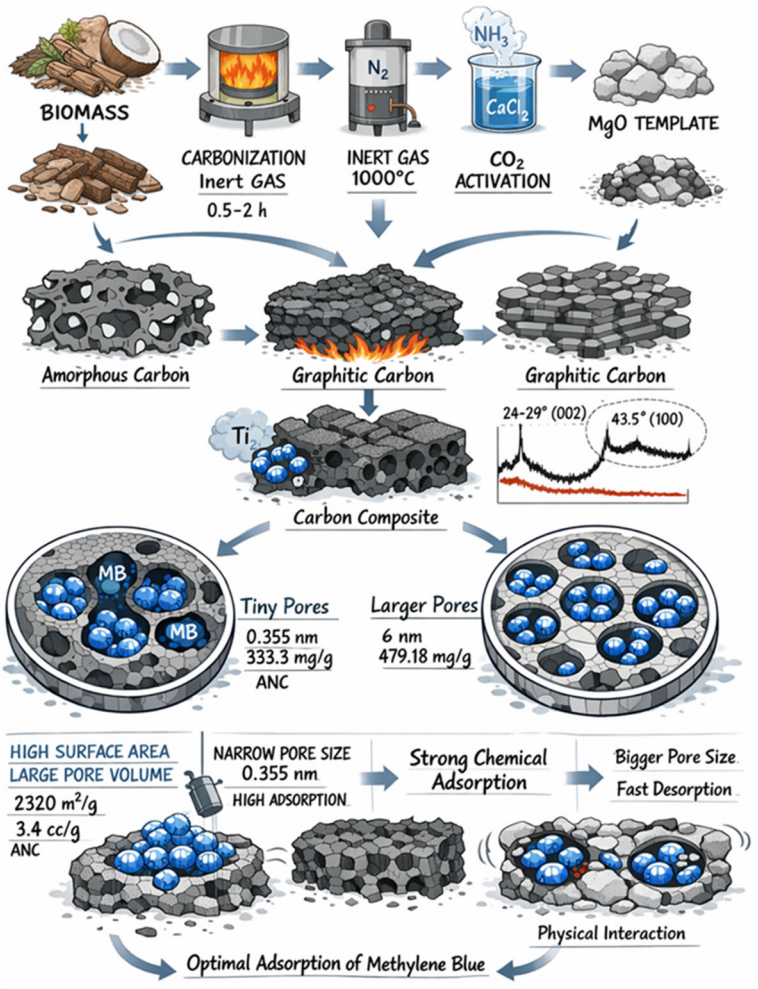

Fig 7. Scheme of carbon production by biomass

porous structure, which increases their MB waste absorption capacity [53-55]. The results of the XRD patterns of carbon samples suggest that the peaks at 24–29.0 (002) and 43.50 (100) are indicative of graphite structure, whereas the broadened spectra indicate that the carbon generated has an amorphous structure. The adsorption capacity reveals that the increase in adsorption capacity is also influenced by the presence of modifiers. Ti-modified AC, whose pore size was lowered from 7 to 6 nm in TiOAC29 due to pore blockage, had capacities of 37.63 and 479.18 mg/g, respectively. Nevertheless, there exist samples with a small pore size and a high adsorption capacity, such as the ANCs sample with a pore size of 0.355 nm and an adsorption capacity of 333.3 mg/g, whereas the CGM sample has a little lower adsorption capacity of 216.33 mg/g. The large surface area and pore volume of ANC, which reached 2320 m^2/g and 3.4 cc/g, respectively, proved to be the primary cause, whereas the surface area and pore volume of CGM were only 69 m^2/g and 0.03 c/g. The narrow pore size of ANCs makes chemical adsorption more likely than CGM interaction with MB. This makes sense since chemical adsorption permits the adsorbent to build chemical connections with MB over a relatively lengthy period, with little chance of the bound MB molecules escaping [56-60]. Possibility 2: MB molecules are imprisoned in microscopic holes, which restricts the desorption of MB molecules due to steric confinement, resulting in a high adsorption capacity [61-64]. In contrast to adsorbents with large pore sizes and limited surface areas, adsorption will occur rapidly because some MB molecules interact physically and have the potential to release bonds at a rapid rate [65-67]. This is also reinforced by the fact that the pore size is excessively big, allowing MB to return to the solution before equilibrium is reached after reacting with the adsorbate. From this phenomenon, it can be concluded that high surface area and high pore volume are still the primary factors in the adsorption of MB, whereas pore size is a secondary factor; pore size that is close to the size of MB (0.9–1.2 nm) has the potential to produce adsorption with a high capacity [68-72].

Carbon Structural Parameters

Carbon's ability to be changed or combined with other elements to create diverse composites is a benefit [73-75]. However, adsorption condition parameters are also of major relevance when engineering an effective, efficient, and cost-effective adsorption process [76-78]. Researchers in the years 2020–2022 will work on adsorbents that require the smallest number of adsorbents with the highest initial pollutant concentration in the shortest amount of time and create the maximum adsorption capacity [79-81]. Table 2 presents a detailed analysis of the correlation between surface area, pore diameter, and adsorption efficiency of various carbon-based adsorbents. The specific surface area (SBET) and pore diameter (D) are shown to play critical roles in determining the adsorption performance [82-84], measured in terms of removal efficiency and adsorption capacity (q). For instance, ACHC-KOH (1:1)

Table 2. Correlation between surface area and pore diameter of carbon for adsorption

Samples	S_{BET} (m^2/g)	D (nm)	t (min)	Co (mg/L)	W (mg)	V (mL)	Removal (%)	q (mg/g)	Ref
OSL (rice husks)	2790.00	1.50	960	300	1000	10	99.00	369.30	[1]
PhAC (reed stalks)	1330.00	2.10	960	300	1000	10	88.65	265.95	[1]
PSL (pine sawdust)	2305.00	1.80	960	300	1000	10	88.65	265.95	[1]
TAL (wheat straw)	1755.00	1.90	960	300	1000	10	71.48	357.38	[1]
GPC-N (*Lycium chinense*)	730.63	4.03	120	140	20	50	99.50	496.53	[2]
GPC-Mg (*Lycium chinense*)	281.53	4.82	120	140	20	50	96.40	48.06	[2]
CSAC (coconut shell)	2228.00	2.50	270	400	200	100	98.00	**658.20**	[3]
CNS-AC (coconut shell)	678.80	1.60	120	100	25	250	99.80	182.48	[4]
S. cumini (guava leaf)	1340.66	2.25	90	100	50	100	95.00	375.61	[5]
KCS (pal kernel shell)	32.21	1.20	180	200	100	50	89.00	45.00	[6]

and ACHC-KOH (1 M), with SBET values of 743. and 703.9 m^2/g, respectively, demonstrate relatively high adsorption capacities (314.05 and 357.38 mg/g). These results suggest that activating agents, such as KOH, and their concentration significantly influences pore structure and adsorption behavior.

Materials with exceptionally high surface areas, such as ANC (2132.1 m^2/g) and IUAC (1486.3 m^2/g), achieve near-complete removal efficiencies (~99 and 99.71%) and high adsorption capacities (369.3 and 344.83 mg/g). These outcomes highlight the importance of optimizing pore structure and specific surface area to enhance adsorbent performance. In contrast, adsorbents with lower surface areas, such as OLPAC (168 m^2/g), show reduced adsorption capacity (38 mg/g) despite a high pore diameter of 5.18 nm, indicating that surface chemistry and pore size distribution must also align with the target contaminant properties for effective adsorption.

Furthermore, materials such as TWAC (878.63 m^2/g) and PC5A8 (206 m^2/g) exhibit high removal efficiencies (88.65 and 87%, respectively), with adsorption capacities dependent on factors beyond surface area, such as contact time (t) and contaminant concentration (Co). This highlights the interplay of physicochemical characteristics and operational conditions in driving adsorption efficacy [82-84]. The results underscore the potential of advanced carbon materials for environmental applications, particularly in water purification, where tailoring surface properties to match specific pollutants can yield optimal performance [85-87].

Table 2 and Fig. 8–9 present a comprehensive overview of the relationship between adsorption conditions and MB removal using various biomass-derived activated carbons reported between 2020 and 2022. As shown in these data, adsorbents with relatively high surface area and well-developed pore structures, such as OSL (rice husks), CSAC (coconut shell), and GPC-N (*Lycium chinense*), exhibited superior MB removal efficiencies, reaching 98.0–99.8%, accompanied by high adsorption capacities (369–658 mg/g). In particular, CSAC demonstrated the highest adsorption capacity (≈658 mg/g) with an efficiency of approximately 98%, highlighting the important role of surface area and pore accessibility in enhancing dye uptake. In contrast, materials with lower surface area, such as KCS (palm kernel shell) and GPC-Mg, showed lower adsorption capacities (≈45–48 mg/g), despite achieving moderate to high removal efficiencies (89–96%). This indicates that removal efficiency alone does not necessarily correlate with adsorption capacity, as the latter is strongly influenced by adsorbent dosage, initial dye concentration, and surface functional groups [88-89].

Modified carbons, especially GPC-N, exhibited remarkably high adsorption performance (q_e ≈497 mg/g with 99.5% removal) even at relatively low adsorbent dosages, which can be attributed to the presence of nitrogen-containing functional groups. These groups enhance electrostatic attraction and π–π interactions between MB molecules and the carbon surface, thereby improving adsorption capacity [90-91]. However, such

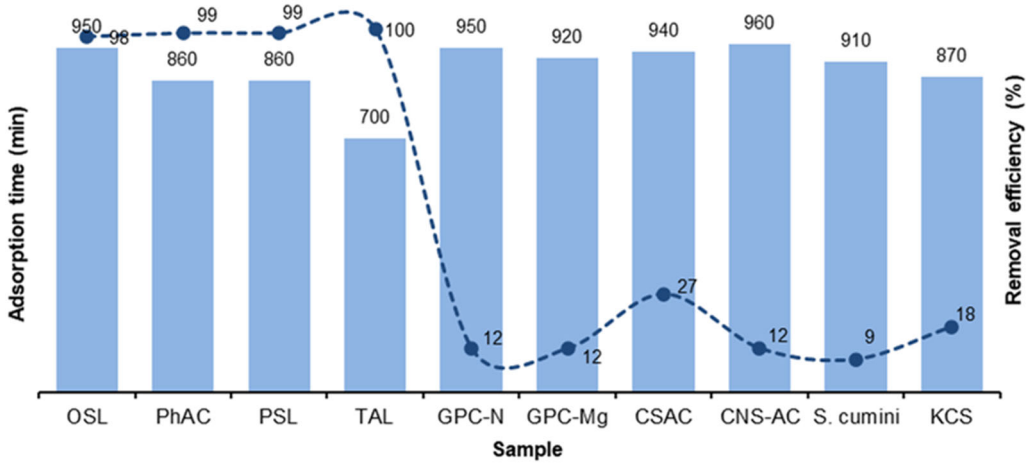

Fig 8. Comparison of adsorption time and removal efficiency for different adsorbents

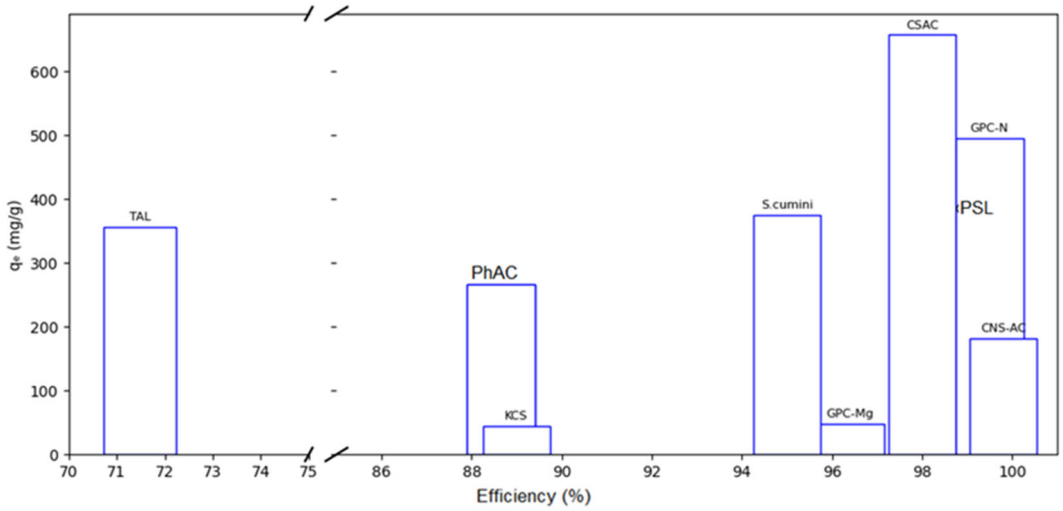

Fig 9. Correlation of percent removal with carbon-based adsorption capacity

materials generally require longer contact times compared to conventional biomass carbons. From a practical perspective, adsorbents such as CNS-AC, SC (*Syzygium cumini*), and OSL offer a favorable balance between adsorption capacity (≈180–376 mg/g), high removal efficiency (>95%), and relatively short contact times, making them more attractive for large-scale wastewater treatment applications. The adsorption times reported in these studies ranged from 90 to 960 min, with most systems achieving equilibrium within a few hours, which is advantageous in terms of energy consumption and operational cost.

Furthermore, the initial dye concentration (C_0), typically ranging from 20 to 500 mg/L, plays a crucial role in determining adsorption capacity. Higher initial concentrations generally resulted in increased q_e values due to a stronger driving force for mass transfer. Nevertheless, excessively high concentrations may require longer contact times or higher adsorbent dosages to maintain high removal efficiency. Overall, the results summarized in Table 2 and Fig. 8–9 confirm that adsorption performance is governed not only by surface area and pore size but also by surface chemistry and synthesis strategy. Different biomass sources and modification routes significantly influence the textural properties and functional groups of the adsorbents, ultimately determining their effectiveness in MB removal.

Carbon synthesis method

Table 3 summarizes the synthesis methods employed for MB removal using various carbon-based adsorbents, highlighting the strong influence of precursor selection, synthesis route, and activation strategy on q_{max} and removal efficiency. The reported methods range from hydrothermal and solvothermal synthesis to impregnation–pyrolysis, spray pyrolysis, and chemical vapor deposition, each designed to tailor the structural and surface properties of the resulting carbon materials. Among the listed samples, nitrogen-modified carbons consistently exhibit superior adsorption performance. GPC-N, synthesized via impregnation and pyrolysis of *Lycium chinense* stalks with ammonium chloride, achieved a high q_{max} of 496.53 mg/g and an excellent removal efficiency of 99.5%. Similarly, N-DAC, produced through hydrothermal treatment followed by nitrogen doping of sawdust, showed a q_{max} of 512.4 mg/g with 96.8% MB removal. These results emphasize the critical role of nitrogen-containing functional groups in enhancing electrostatic attraction and π–π interactions between MB molecules and the carbon surface.

Activation strategies also play a decisive role in improving adsorption performance. SUK-113, prepared via one-step KOH and urea activation of sucrose, demonstrated a remarkably high q_{max} of 618.5 mg/g with

Table 3. Synthesis method for MB removal

Sample	Method	Precursor	Aging time (min)	Carbonization temp (°C)	Template	q_{max} (mg/g)	% Removal	Ref
GPC-N	Impregnation and pyrolysis	*Lycium chinense* stalk + NH_4Cl	120	900	Ammonium chloride	496.53	99.50	[2]
AC-glucose-KOH	Hydrothermal treatment + KOH activation	Glucose	180	600	Surfactant (implicit)	356.80	89.40	[7]
BDSS	Pyrolysis + chemical activation	Durian peel + seed	60	500	None	136.99	91.20	[8]
CNF-Ni-CVD	Chemical vapor deposition	Polyacrylonitrile + graphite	ND	650	Alumina membrane	458.20	94.60	[9]
N-DAC	Hydrothermal + nitrogen doping	Sawdust + hydrothermal	120	700	Sawdust	512.40	96.80	[10]
CS-aerogel-Zn	Freeze-drying + carbonization	Chitosan + zinc acetate	1440 (24 h)	700	Zinc chloride	441.60	93.50	[11]
SUK-113	One-step KOH + urea activation	Sucrose + urea	ND	800	KOH	618.50	98.30	[12]
CQD-solvothermal	Solvothermal synthesis	Glucose + ethylene glycol	180	400	Ethylene glycol	327.40	87.20	[13]
CQD/TNT-hydrothermal	Hydrothermal + calcination	Glucose + TiO_2	4320 (72 h)	550	Microsphere polystyrene	445.20	91.80	[14]
NP-CQD-hydrothermal	Single-step Hydrothermal	Citric acid + urea	ND	200	None	483.60	93.73	[15]
CSAC-spray-pyrolysis	Spray pyrolysis	Sucrose + sodium bicarbonate	180	1000	Sodium bicarbonate	658.20	98.00	[16]

a removal efficiency of 98.3%, confirming the effectiveness of combined chemical activation and heteroatom doping. Likewise, CSAC synthesized by spray pyrolysis using sucrose and $NaHCO_3$ reached the highest adsorption capacity among the listed samples (658.2 mg/g) with 98.0% removal, which can be attributed to high carbonization temperature (1000 °C) and *in situ* pore generation induced by the activating agent. In contrast, adsorbents synthesized without extensive chemical activation or templating, such as BDSS derived from durian peel and seed, exhibited lower adsorption capacity (136.99 mg/g), despite maintaining relatively high removal efficiency (91.2%). This indicates that removal percentage alone does not fully reflect adsorption performance, as q_{max} is strongly governed by pore development and surface chemistry.

Carbon nanostructured materials synthesized via advanced routes also show promising performance. CNF-Ni-CVD, obtained by chemical vapor deposition using polyacrylonitrile and graphite with an alumina membrane template, achieved a q_{max} of 458.2 mg/g and 94.6% removal efficiency. Similarly, carbon quantum dot–based adsorbents prepared via hydrothermal or solvothermal methods, such as NP-CQD-Hydrothermal and CQD/TNT-Hydrothermal, demonstrated q_{max} values of 445–484 mg/g, although often requiring longer aging times to achieve optimal performance. Overall, the data in Table 3 clearly demonstrate that synthesis method, activation route, and heteroatom incorporation collectively determine the adsorption behavior of carbon-based materials toward MB. High carbonization temperatures, appropriate chemical activation, and nitrogen doping are particularly effective in enhancing adsorption capacity while maintaining high removal efficiency. These findings underline the importance of rational synthesis design in developing high-performance and scalable adsorbents for wastewater treatment applications.

Parameter adsorption and its kinetic study

Fig. 10 illustrates the trend of adsorption capacity (q_e) of MB on various carbon-based adsorbents as evaluated using the pseudo-second-order (PSO) kinetic model. As summarized in Table 4, the experimental data for most samples exhibit a strong agreement with the PSO model, as indicated by high coefficients of determination (R^2 ranging from 0.858 to 0.998). This suggests that the adsorption process is predominantly governed by chemisorption involving electron sharing or exchange between MB molecules and the active sites of the carbon materials. Among the evaluated adsorbents, PC-900 demonstrates the highest adsorption capacity, with a calculated q_e of 1570.1 mg/g and an experimental value of 1554.32 mg/g, accompanied by an excellent R^2 value of 0.998. This superior performance can be attributed to the high carbonization temperature (900 °C), which likely enhances pore development and surface reactivity. Similarly, BAC-750-90 also exhibits a high adsorption capacity (q_e = 561.79 mg/g) with good agreement between calculated and experimental values, confirming the suitability of the PSO model for describing its adsorption kinetics.

$$\frac{t}{q_t} = \frac{1}{k_2 q_e^2} + \frac{1}{q_e} \quad (1)$$

The effect of initial MB concentration (C_0) on adsorption capacity is clearly observed in the GO@CA series. As C_0 increases from 50 to 200 mg/L, the adsorption capacity progressively rises from 122.46 to 316.56 mg/g. Although the rate constant (k) slightly decreases with increasing concentration, the overall adsorption capacity improves, indicating that higher driving forces at elevated concentrations promote greater dye uptake. This trend is consistent with the adsorption capacity profiles depicted in Fig. 10. In contrast, ACS-40 and ACS-120 exhibit relatively low adsorption capacities (7.09 and 13.95 mg/g, respectively), despite having comparatively higher rate constants. This behavior suggests that these materials favor faster adsorption kinetics but possess limited active sites or surface area for MB uptake. The close correspondence between calculated and experimental q_e values and the high R^2 values (>0.995) further confirm the validity of the PSO model for these systems.

The adsorption kinetics are also influenced by operational parameters such as contact time, adsorbent dosage, and solution volume. Most carbon adsorbents in Table 4 require extended contact times, typically between

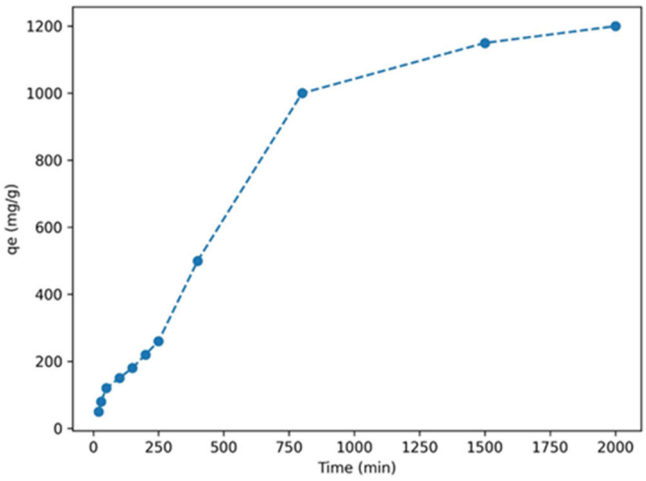

Fig 10. The trend of adsorption capacity

Table 4. Kinetic model PSO of MB adsorption on carbon

Samples	k (g/mg/min)	q_e (mg/g)	q_e exp	R^2	Co (mg/L)	W (mg)	V (mL)	t (min)	Ref
BAC-750-90	4.54×10^{-4}	561.790	560.940	0.945	100	10	50	360	[17]
PC-900	3.10×10^{-5}	1570.100	1554.320	0.998	100	10	200	600	[18]
SU-KOH-500	2.33×10^{-6}	361.000	384.000	0.990	500	15	50	180	[19]
SU-H_3PO_4-200	7.30×10^{-7}	82.000	108.000	0.990	200	10	50	120	[19]
ACS-40	0.0237	7.092	6.324	0.998	40	100	100	60	[20]
ACS-120	0.0039	13.951	9.845	0.995	120	100	100	60	[20]
GO@CA-50	0.0015	122.460	99.440	0.866	50	10	100	600	[21]
GO@CA-100	0.0011	185.220	184.080	0.960	100	10	100	600	[21]
GO@CA-150	0.0009	250.580	248.500	0.957	150	10	100	600	[21]
GO@CA-200	0.0008	316.560	308.200	0.858	200	10	100	600	[21]

3 and 10 h, to reach equilibrium adsorption. This indicates that sufficient interaction time is necessary for MB molecules to fully occupy available adsorption sites, particularly for high-capacity materials such as PC-900 and GO@CA composites. Overall, the kinetic analysis presented in Table 4 and the adsorption trends shown in Fig. 10 highlight the critical role of adsorbent structure, surface chemistry, and initial dye concentration in governing MB removal. The strong conformity to the pseudo-second-order model across different materials underscores the dominance of chemisorption mechanisms and provides valuable insight for optimizing carbon-based adsorbents for efficient dye removal in wastewater treatment applications.

Regeneration

Table 5 summarizes the regeneration performance of various carbon-based adsorbents after MB adsorption, highlighting their reusability across multiple adsorption–desorption cycles. Regeneration efficiency is a key indicator of adsorbent sustainability and operational feasibility, as it reflects the material's ability to maintain adsorption capacity after repeated use. The table shows that most studies evaluated regeneration up to five cycles, with removal efficiencies generally decreasing as the number of cycles increased. Solvent-based batch regeneration is the most widely applied method, utilizing solvents such as ethanol, deionized water, NaOH, and HCl. Among ethanol-regenerated materials, AC-GW, EFAC, and Ni/Al-GO exhibit relatively high initial removal efficiencies, exceeding 87% in the first cycle. However, their performance gradually declines with subsequent cycles, indicating partial loss of active sites or incomplete desorption of MB. Notably, Ni/Al-GO demonstrates excellent regeneration stability, retaining more than 93% removal efficiency even after the fifth cycle, suggesting strong structural integrity and effective solvent-assisted desorption.

Water-based regeneration methods, as observed for AC-CS and Mg@FA, also show good regeneration performance, with first-cycle removal efficiencies above 90%. Nevertheless, a more pronounced decline is observed after multiple cycles, particularly for Mg@FA, where removal efficiency drops to 54.18% by the fifth cycle. This reduction may be attributed to the weaker desorption capability of water compared to organic solvents or the gradual degradation of adsorption sites. Chemical regeneration using acidic or alkaline solutions presents mixed results. FCBAC regenerated with NaOH shows a steady decrease in efficiency from 90% in the first

Table 5. Regeneration carbon after MB adsorption

Samples	Regeneration method	Solvent	Regeneration condition	% Removal in Cycles					Ref.
				1st	2nd	3rd	4th	5th	
AC-GW	Solvent batch	95% Ethanol	Shaker 200 rpm, 4 h, 110 °C drying	98.00	89.00	78.00	72.00	65.00	[22]
EFAC	Solvent batch	Ethanol (90%)	25 °C, 4 h, shaking at 200 rpm	87.10	85.50	84.20	ND	ND	[23]
FCBAC	Solvent batch	NaOH	100 rpm, 60 min, distilled water wash	90.00	82.00	71.00	60.00	45.00	[24]
AC-CS	Solvent batch	Deionized water	Thermal holding 25 °C, wash and dry	90.77	85.40	78.60	70.20	62.10	[25]
Mg@FA	Adsorption-desorption cycle	Deionized water	Room temperature, 1 h stirring for desorption	95.61	90.40	85.70	80.50	54.18	[26]
GO/DETA/$MnFe_2O_4$@SiO_2	Solvent batch + magnetic separation	0.1 M HCl	Room temperature, magnetic extraction, multiple cycles	99.20	96.80	92.50	74.00	ND	[27]
Zn-BC-600	Thermal regeneration	ND	Heating 500 °C in N_2 atmosphere, 1 h	91.80	88.50	85.20	82.10	78.40	[28]
GO/CS	Thermal + ultrasound + chemical	Ethanol 70%, NaCl 1 M, DI water	40-80 °C, ultrasound, 1-6 h contact time	99.10	97.40	95.80	93.20	90.50	[29]
Ni/Al-GO	Solvent Batch	Ethanol	Room temperature, magnetic separation possible	97.37	96.20	94.80	94.10	93.49	[30]
Fe_3O_4@SiO_2@La	Magnetic Separation + Chemical Desorption	2 M HCl	pH 10, 70 min contact, magnetic field extraction	96.50	94.20	91.80	88.90	85.30	[31]

cycle to 45% in the fifth, indicating possible structural damage or pore blockage from repeated chemical exposure. In contrast, Fe_3O_4@SiO_2@La regenerated with 2 M HCl maintains relatively high removal efficiencies, remaining above 85% after five cycles. The presence of magnetic components facilitates efficient separation and minimizes material loss during regeneration, contributing to improved long-term performance.

Thermal regeneration, represented by Zn-BC-600, demonstrates a comparatively stable regeneration trend, with removal efficiency decreasing gradually from 91.8 to 78.4% over five cycles. Although thermal treatment effectively removes adsorbed dye, it requires high energy input and may alter the carbon microstructure, which can ultimately limit adsorption performance over extended cycles.

Hybrid regeneration approaches combining solvent treatment with magnetic separation, such as GO/DETA/$MnFe_2O_4$@SiO_2, show outstanding regeneration efficiency in early cycles, with removal exceeding 92% up to the third cycle. However, data for later cycles are not available, indicating a need for further long-term evaluation. Overall, the data in Table 5 demonstrate that regeneration performance is strongly influenced by both the regeneration method and the structural characteristics of the carbon-based adsorbents. Solvent batch regeneration, particularly using ethanol, appears to be the most effective and widely adopted approach, as it enables efficient desorption while minimizing damage to the carbon structure. Additionally, materials incorporating magnetic components or metal oxides exhibit enhanced regeneration stability due to improved structural robustness and ease of recovery. These findings emphasize that selecting an appropriate regeneration strategy tailored to the adsorbent's structural and textural properties is crucial for maintaining high MB removal efficiency over multiple cycles.

The interaction between MB and carbon-based adsorbents (Fig. 11), as reflected in the regeneration data presented in Table 5, is governed by a combination of physical and chemical mechanisms. These include pore-filling adsorption within the carbon micro- and mesoporous structure, electrostatic interactions between the cationic MB molecules and negatively charged functional groups on the carbon surface (such as carboxyl and hydroxyl groups), π–π interactions between the aromatic rings of MB and the graphitic domains of carbon, as well as weaker Van der Waals forces. The effectiveness of these interactions is indirectly demonstrated by the ability of the adsorbents to retain high removal efficiencies over multiple regeneration cycles. The regeneration performance shown in Table 5 indicates that solvent-based regeneration, particularly using ethanol and deionized water, is effective in disrupting these interactions without causing severe

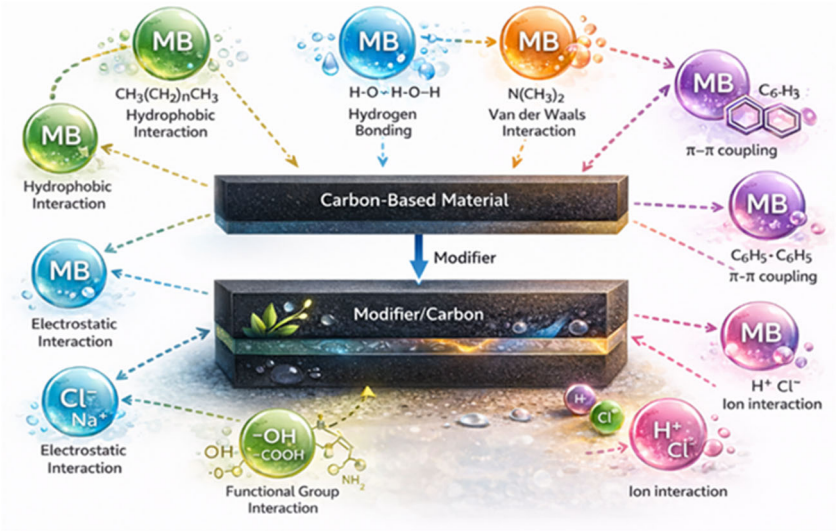

Fig 11. The mechanism of the reaction between MB and carbon adsorbents

damage to the carbon structure. Ethanol regeneration, for example, facilitates desorption by weakening electrostatic attractions and π–π interactions through its polarity, enabling efficient removal of residual MB from adsorption sites. This is evidenced by materials such as Ni/Al-GO and GO/CS, which maintain removal efficiencies above 90% even after five cycles, indicating strong reversibility of the adsorption mechanism and high structural stability.

In contrast, regeneration methods involving strong chemical agents or high-temperature thermal treatment tend to show a more pronounced decline in adsorption efficiency with increasing cycles. The gradual reduction in removal efficiency observed for materials regenerated using NaOH or thermal treatment suggests partial degradation of surface functional groups, pore blockage, or alteration of the carbon microstructure. These changes reduce the availability of active adsorption sites, thereby weakening the adsorption mechanisms in subsequent cycles. Furthermore, the incorporation of modifiers such as metal oxides or magnetic components, as seen in Fe_3O_4@SiO_2@La and GO/DETA/$MnFe_2O_4$@SiO_2, enhances regeneration stability by improving structural robustness and facilitating efficient recovery during desorption. The sustained regeneration performance of these materials indicates that strong initial adsorption mechanisms can be balanced with effective desorption when the material structure is appropriately engineered. Overall, the data in Table 5 demonstrate that the adsorption–desorption mechanism of MB on carbon-based materials is highly dependent on the preservation of surface functional groups and pore structure during regeneration. Effective regeneration methods are those that selectively disrupt dye–adsorbent interactions while maintaining the integrity of the carbon framework. These findings highlight the importance of aligning regeneration strategy with the underlying adsorption mechanism and material structure to ensure long-term reusability and practical applicability in wastewater treatment systems.

The publication trends regarding the synthesis of materials for MB removal indicate a significant surge in research interest over recent years (Fig. 12). As evidenced by the steadily increasing number of publications in recent years, the scientific community is rapidly recognizing the critical role of advanced materials in solving environmental challenges. This upward trend emphasizes the urgency with which researchers are developing innovative solutions to remove pollutants, like MB, from wastewater, highlighting the growing concerns about environmental contamination and the need for effective remediation strategies.

The publication trend related to the synthesis of materials for MB removal shows a clear and consistent increase from 2005 to 2025, reflecting a steadily growing research interest in this field (Fig. 13). In the early period (2005–2010), the number of publications increased gradually, indicating an initial exploratory phase in which researchers began to recognize the potential of material-based approaches for dye removal. This phase

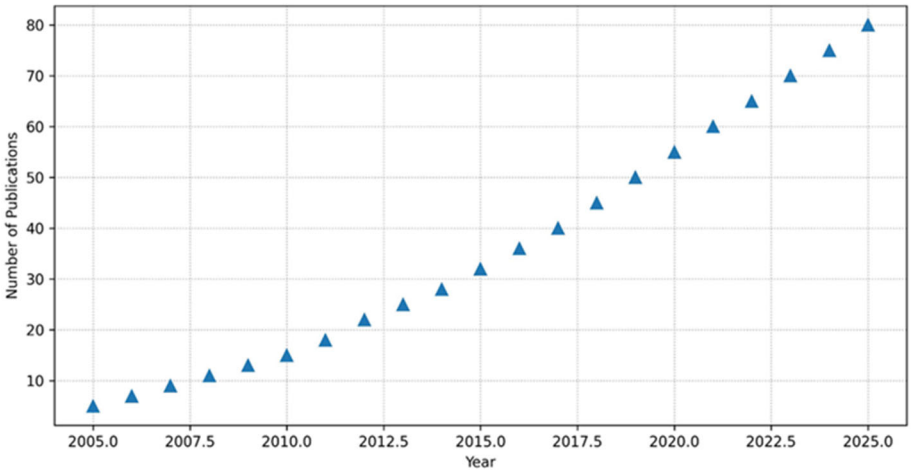

Fig 12. Tren publication of MB

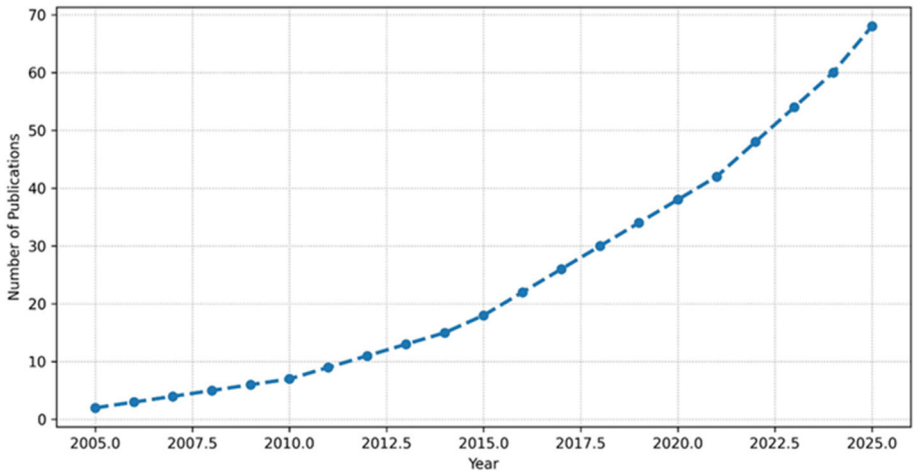

Fig 13. Tren publication of synthesis material for MB removal

was followed by a more pronounced growth after 2010, with a noticeable acceleration from around 2015 onward, suggesting a transition toward more intensive and application-oriented research. The sharp rise in publications in recent years highlights the increasing urgency of addressing wastewater pollution, particularly from synthetic dyes such as MB [88-89]. This trend underscores the growing awareness within the scientific community of the critical role that advanced functional materials play in environmental remediation. The focus has progressively shifted toward the development of materials with higher adsorption capacities, improved structural stability, and enhanced regeneration performance, which are essential for achieving efficient and sustainable dye removal processes [90-91].

Furthermore, the diversity of synthesis strategies reported in the literature—including hydrothermal, sol–gel, and hard-template methods—illustrates the adaptability of material design to meet different operational and environmental requirements. Such versatility is crucial for scaling up laboratory findings toward practical and industrial applications. Overall, the upward publication trend reflects not only increasing research activity but also the maturation of this field toward more robust, efficient, and application-ready materials for MB removal. Looking ahead, the sustained growth in research output suggests strong future prospects for material-based wastewater treatment technologies [92-93]. As global water contamination continues to intensify due to industrialization and urban expansion, continued innovation in material synthesis is expected to play a pivotal role in developing scalable and long-term solutions for water purification [94-96]. Consequently, this research area is likely to remain a key focus in environmental materials science and sustainable water treatment technologies.

■ CONCLUSION

In conclusion, the relentless challenge of MB contamination in water bodies is being met with innovative solutions, particularly using carbon-based materials. These materials, especially those derived from biomass, have emerged as promising contenders for efficient and cost-effective water purification. The remarkable surface area and porosity of biomass-derived carbons, such as those obtained from *Areca catechu* nut powder and soybean dregs, significantly enhance their adsorption capacity, making them highly effective in removing MB. Pyrolysis conditions, including temperature and time, play a crucial role in optimizing these properties, enabling the development of adsorbents with tailored characteristics to maximize pollutant removal. The versatility of carbon-based materials is further enhanced by modifications that incorporate advanced functional groups and composites, improving their adsorption efficiency. For instance, the integration of metal oxides like TiO_2 and ZnO with carbon materials has not only increased photocatalytic activity but also

addressed issues such as electron recombination, setting new benchmarks for the efficiency of MB degradation. Graphene, a high-surface-area material, is also making waves in the field due to its exceptional adsorption properties, paving the way for large-scale applications in water treatment. As the field progresses, the interplay between green chemistry principles, nanotechnology, and material science continues to unlock new potential. The growing body of research on carbon-based adsorbents not only offers sustainable solutions to the global water pollution crisis but also exemplifies the innovative strides being made towards cleaner, healthier ecosystems for future generations.

■ ACKNOWLEDGMENTS

This research is funded by the Indonesian Endowment Fund for Education (LPDP) on behalf of the Indonesian Ministry of Higher Education, Science and Technology and managed under the EQUITY Program of Universitas Sebelas Maret (Contract No. 4315/B3/DT.03.08/2025 and No. 84/UN27/KS/2025) in the scheme of Hibah International Research Network Program EQUITY The Impact Rankings 2025.

■ CONFLICT OF INTEREST

The authors declare no conflict of interest.

■ AUTHOR CONTRIBUTIONS

Conceptualization: Maria Ulfa; methodology: Maria Ulfa and Ayu Tri Rahmawati; software: Rizka Fauzia Hanif; formal analysis: Maria Ulfa, Cindy Nur Anggreani, and Rizka Fauzia Hanif; investigation: Maria Ulfa and Cindy Nur Anggreani; data curation: Ayu Tri Rahmawati and Rizka Fauzia Hanif; writing—original draft preparation: Maria Ulfa, Ayu Tri Rahmawati, and Cindy Nur Anggreani; writing—review and editing: Maria Ulfa and Rizka Fauzia Hanif; visualization: Cindy Nur Anggreani; supervision, project administration, and funding acquisition: Maria Ulfa. All authors have read and agreed to the published version of the manuscript.

■ REFERENCES

[1] Sabitov, A., Atamanov, M., Doszhanov, O., Saurykova, K., Tazhu, K., Kerimkulova, A., Orazbayev, A., and Doszhanov, Y., 2024, Surface characteristics of activated carbon sorbents obtained from biomass for cleaning oil-contaminated soils, *Molecules*, 29 (19), 3786.

[2] Ren, Y., Geng, W., Xu, R., Wang, P., and Zhao, H., 2025, Tuning electronic and pore structures of biochar via nitrogen and magnesium doping for superior methylene blue adsorption: Synergistic mechanisms and kinetic analysis, *ACS Omega*, 10 (29), 31679–31692.

[3] Wang, Y., Duan, Y., Liang, X., Tang, L., Sun, L., Wang, R., Wei, S., Huang, H., Yang, P., and Hu, H., 2023, Hierarchical porous activated carbon derived from coconut shell for ultrahigh-performance supercapacitors, *Molecules*, 28 (20), 7187.

[4] Hoc Thang, N., Sy Khang, D., Duy Hai, T., Thi Nga, D., and Dinh Tuan, P., 2021, Methylene blue adsorption mechanism of activated carbon synthesised from cashew nut shells, *RSC Adv.*, 11 (43), 26563–26570.

[5] Amiry, R.M., Mwankuna, C.J., Mariki, E.E., and Mkoma, S.L., 2025, Optimization and characterization of high surface area mesoporous activated carbon produced from *Syzygium cumini* leaves bio-waste by zinc chloride activation, *Next Res.*, 2 (2), 100219.

[6] Zakir, M., Taba, P., Permatasari, N.U., and Nurdin, M., 2025, Palm kernel shell based hydrothermal carbon for methylene blue removal in wastewater treatment: Application of dual adsorption isothermal models, *J. Ecol. Eng.*, 26 (7), 394–407.

[7] Appiah, F.A., Nugloze, D., Sai-Obodai, L.S., Natewong, P., and Idem, R.O., 2023, Activated carbon produced from the hydrothermal treatment of glucose with KOH activation for catalytic absorption of CO_2 in a BEA-AMP Bi-solvent blend, *ACS Omega*, 8 (10), 9346–9355.

[8] Huong, D.T., Ngan, N.N.P., Anh, D.T.T., Vinh, N.D., and Xuan, V.T., 2025, Durian peel–seed biochar for efficient methylene blue removal from water: Synthesis, characterization, and adsorption performance, *RSC Adv.*, 15 (40), 33726–33749.

[9] Albetran, H.M., 2023, Synthesis and characterization

of electrospun carbon nanofibers from polyacrylonitrile and graphite nanoplatelets, *Materials*, 16 (4), 1749.

[10] El Nemr, M.A., Hassaan, M.A., and Ashour, I., 2023, Formation of self-nitrogen-doping activated carbon from Fish/sawdust/$ZnCl_2$ by hydrothermal and pyrolysis for toxic chromium adsorption from wastewater, *Sci. Rep.*, 13 (1), 11556.

[11] Hu, J., Zhao, C., Si, Y., Hong, C., Xing, Y., Wang, Y., Ling, W., Feng, W., and Feng, L., 2023, Preparation of ultrafine microporous nitrogen self-doped chitosan (CS) carbon aerogel based on a Zn-Zn system for high-performance supercapacitors, *Appl. Surf. Sci.*, 637, 157910.

[12] Hakami, O., 2023, Urea-doped hierarchical porous carbons derived from sucrose precursor for highly efficient CO_2 adsorption and separation, *Surf. Interfaces*, 37, 102668.

[13] Chávez-García, D., Guzman, M., Sanchez, V., and Cadena-Nava, R.D., 2024, Green synthesis of biomass-derived carbon quantum dots for photocatalytic degradation of methylene blue, *Beilstein J. Nanotechnol.*, 15, 755–766.

[14] Rawat, J., Dwivedi, C., and Sharma, P., 2025, Photocatalytic degradation of methylene blue and tetracycline under visible light by fabricated carbon quantum dot decorated TiO_2 nanotubes, *Nanocomposites*, 11 (1), 137–150.

[15] Shi, B., Su, Y., Zhang, L., Huang, M., Liu, R., and Zhao, S., 2016, Nitrogen and phosphorus Co-doped carbon nanodots as a novel fluorescent probe for highly sensitive detection of Fe^{3+} in human serum and living cells, *ACS Appl. Mater. Interfaces*, 8 (17), 10717–10725.

[16] Min, B.H., and Jung, K.Y., 2017, Improved porosity and ionic sorption capacity of carbon particles prepared by spray pyrolysis from an aqueous sucrose/$NaHCO_3$/TEOS solution, *RSC Adv.*, 7 (34), 21314–21322.

[17] He, Y., Ni, L., Gao, Q., Ren, H., Su, M., Hou, Y., and Liu, Z., 2023, Activated carbon with ultrahigh specific surface derived from bamboo shoot shell through K_2FeO_4 oxidative pyrolysis for adsorption of methylene blue, *Molecules*, 28 (8), 3410.

[18] Wang, S., Dou, J., Zhang, T., Li, S., and Chen, X., 2023, Selective adsorption of methyl orange and methylene blue by porous carbon material prepared from potassium citrate, *ACS Omega*, 8 (38), 35024–35033.

[19] Liyanaarachchi, H., Thambiliyagodage, C., Lokuge, H., and Vigneswaran, S., 2023, Kinetics and thermodynamics study of methylene blue adsorption to sucrose- and urea-derived nitrogen-enriched, hierarchically porous carbon activated by KOH and H_3PO_4, *ACS Omega*, 8 (18), 16158–16173.

[20] Abbas, M., and Trari, M., 2024, Adsorption behavior of methylene blue onto activated coconut shells: kinetic, thermodynamic, mechanism and regeneration of the adsorbent, *Dose-Response,* 22 (4), 15593258241290708.

[21] Eltaweil, A.S., Abd El-Monaem, E.M., El-Subruiti, G.M., Ali, B.M., Abd El-Latif, M.M., and Omer, A.M., 2023, Graphene oxide incorporated cellulose acetate beads for efficient removal of methylene blue dye; isotherms, kinetic, mechanism and co-existing ions studies, *J. Porous Mater.*, 30 (2), 607–618.

[22] Mousavi, S.A., Shahbazi, D., Mahmoudi, A., and Darvishi, P., 2021, Methylene blue removal using prepared activated carbon from grape wood wastes: adsorption process analysis and modeling, *Water Qual. Res. J.*, 57 (1), 1–19.

[23] Li, H., Liu, L., Cui, J., Cui, J., Wang, F., and Zhang, F., 2020, High-efficiency adsorption and regeneration of methylene blue and aniline onto activated carbon from waste edible fungus residue and its possible mechanism, *RSC Adv.*, 10 (24), 14262–14273.

[24] Pathania, D., Sharma, S., and Singh, P., 2017, Removal of methylene blue by adsorption onto activated carbon developed from *Ficus carica* bast, *Arabian J. Chem.*, 10 (Suppl. 1), S1445–S1451.

[25] Regunton, P.C.V, and Sumalapao, D.E.P., 2018, Biosorption of methylene blue from aqueous solution by coconut (*Cocos nucifera*) shell-derived activated carbon-chitosan composite, *Orient. J. Chem.*, 34 (1), 115–124.

[26] Zhou, J., Li, M., Tao, Y., and Zha, L., 2025, Study on the adsorption characteristics of methylene blue by magnesium-modified fly ash, *Molecules*, 30 (5), 992.

[27] Banaei, A., Saadat, A., Javadi, R., and Pargolghasemi, P., 2024, Preparation magnetic graphene oxide/diethylenetriamine composite for removal of methylene blue from aqueous solutions, *Sci. Rep.*, 14 (1), 15457.

[28] Zhu, W., Chen, F., Ye, L., Yang, X., Song, Y., and Wang, H., 2024, Methylene blue and acid red adsorption on biochar made from modified sugarcane bagasse: A dynamic, equilibrium, and thermodynamic investigation, *Adsorpt. Sci. Technol.*, 42, 02636174241273522.

[29] Luong, H.V.T., Le, T.P., Le, T.L.T., Dang, H.G., and Tran, T.B.Q., 2024, A graphene oxide based composite granule for methylene blue separation from aqueous solution: Adsorption, kinetics and thermodynamic studies, *Heliyon*, 10 (7), e28648.

[30] Amri, A., Wibiyan, S., Wijaya, A., Ahmad, N., Mohadi, R., and Lesbani, A., 2024, Efficient adsorption of methylene blue dye using Ni/Al layered double hydroxide-graphene oxide composite, *Bull. Chem. React. Eng. Catal.*, 19 (2), 181–189.

[31] Yazdizadeh, S., Ebrahimipour, S.Y., Fatemi, S.J., Khaleghi, M., and Ramezanpour, S., 2025, Mesoporous Fe_3O_4@SiO_2@La nanocomposite for efficient methylene blue removal from wastewater, *J. Mol. Struct.*, 1322 (Pt. 1), 140337.

[32] Essa, W.K., Yasin, S.A., Abdullah, A.H., Thalji, M.R., Saeed, I.A., Assiri, M.A., Chong, K.F., and Ali, G.A.M., 2022, Taguchi L25 (5^4) approach for methylene blue removal by polyethylene terephthalate nanofiber-multi-walled carbon nanotube composite, *Water*, 14 (8), 1242.

[33] Safri, A., and Fletcher, A.J., 2022, Effective carbon/TiO_2 gel for enhanced adsorption and demonstrable visible light driven photocatalytic performance, *Gels*, 8 (4), 215.

[34] Feng, Z.Y., and Meng, L.Y., 2021, Hierarchical porous carbons derived from corncob: Study on adsorption mechanism for gas and wastewater, *Carbon Lett.*, 31 (4), 643–653.

[35] Song, G., Shi, Y., Li, A., Wang, H., and Ding, G., 2021, Facile preparation of three-dimensional graphene oxide/ι-carrageenan composite aerogel and its efficient ability for selective adsorption of methylene blue, *J. Mater. Sci.*, 56 (26), 14866–14879.

[36] Kara, S., Aydiner, C., Demirbas, E., Kobya, M., and Dizge, N., 2007, Modeling the effects of adsorbent dose and particle size on the adsorption of reactive textile dyes by fly ash, *Desalination*, 212 (1-3), 282–293.

[37] Udayakumar, M., El Mrabate, B., Koós, T., Szemmelveisz, K., Kristály, F., Leskó, M., Filep, Á., Géber, R., Schabikowski, M., Baumli, P., Lakatos, J., Tóth, P., and Németh, Z., 2021, Synthesis of activated carbon foams with high specific surface area using polyurethane elastomer templates for effective removal of methylene blue, *Arabian J. Chem.*, 14 (7), 103230.

[38] Hachemaoui, M., Boukoussa, B., Mokhtar, A., Mekki, A., Beldjilali, M., Benaissa, M., Zaoui, F., Hakiki, A., Chaibi, W., Sassi, M., and Hamacha, R., 2020, Dyes adsorption, antifungal and antibacterial properties of metal loaded mesoporous silica: Effect of metal and calcination treatment, *Mater. Chem. Phys.*, 256, 123704.

[39] Ulfa, M., Prasetyoko, D., Trisunaryanti, W., Bahruji, H., Fadila, Z.A., and Sholeha, N.A., 2022, The effect of gelatin as pore expander in green synthesis mesoporous silica for methylene blue adsorption, *Sci. Rep.*, 12 (1), 15271.

[40] Zhu, X., Yang, J., Gao, L., Liu, J., Yang, D., Sun, X., Zhang, W., Wang, Q., Li, L., He, D., and Kumar, R.V., 2013, Preparation of lead carbonate from spent lead paste via chemical conversion, *Hydrometallurgy*, 134-135, 47–53.

[41] Minhas, M.B., Jande, Y.A.C., and Kim, W.S., 2014, Combined reverse osmosis and constant-current operated capacitive deionization system for seawater desalination, *Desalination*, 344, 299–305.

[42] Esmaeili, Y., Bidram, E., Zarrabi, A., Amini, A., and Cheng, C., 2020, Graphene oxide and its derivatives as promising *in-vitro* bio-imaging platforms, *Sci. Rep.*, 10 (1), 18052.

[43] Simonescu, C.M., Culita, D.C., Tatarus, A., Mocanu, T., Marinescu, G., Mitran, R.A., Atkinson, I., Kuncser, A., and Stanica, N., 2022, Novel magnetic nanocomposites based on carboxyl-functionalized SBA-15 silica for effective dye adsorption from aqueous solutions, *Nanomaterials*, 12 (13), 2247.

[44] Galaburda, M., Bosacka, A., Sternik, D., Bogatyrov, V., Oranska, O., Gun'ko, V., and Deryło-Marczewska, A., 2022, Development, synthesis and characterization of tannin/bentonite-derived biochar for water and wastewater treatment from methylene blue, *Water*, 14 (15), 2407.

[45] Chai, Y.D., Pang, Y.L., Lim, S., and Chong, W.C., 2021, Sonocatalytic degradation of Congo Red using biomass-based cellulose/TiO_2 composite, *Mater. Today: Proc.*, 42 (Pt. 1), 50–55.

[46] Dao, M.U., Nguyen, T.T.T., Le, V.T., Hoang, H.Y., Le, T.T.N., Pham, T.N., Nguyen, T.T., Akhmadullin, R.M., Le, H.S., Tran, H.V., and Tran, D.L., 2021, Non-woven polyester fabric-supported cuprous oxide/reduced graphene oxide nanocomposite for photocatalytic degradation of methylene blue, *J. Mater. Sci.*, 56 (17), 10353–10366.

[47] Joshi, S., Shrestha, R.G., Pradhananga, R.R., Ariga, K., and Shrestha, L.K., 2022, High Surface area nanoporous activated carbons materials from *Areca catechu* nut with excellent iodine and methylene blue adsorption, *C*, 8 (1), 2.

[48] Dai, Z., Ren, P.G., Zhang, H., Gao, X., and Jin, Y.L., 2021, Nitrogen-doped and hierarchically porous carbon derived from spent coffee ground for efficient adsorption of organic dyes, *Carbon Lett.*, 31 (6), 1249–1260.

[49] Ying, Z., Huang, L., Ji, L., Li, H., Liu, X., Zhang, C., Zhang, J., and Yi, G., 2021, Efficient removal of methylene blue from aqueous solutions using a high specific surface area porous carbon derived from soybean dreg, *Materials*, 14 (7), 1754.

[50] Chen, Q., Wang, H., Tang, X., Ba, Z., Zhao, X., Wang, Y., and Deng, H., 2021, One-step synthesis of carbon quantum dot-carbon nanotube composites on waste eggshell-derived catalysts for enhanced adsorption of methylene blue, *J. Environ. Chem. Eng.*, 9 (5), 106222.

[51] Ahmad, M.A., Mohamad Yusop, M.F., Zakaria, R., Karim, J., Yahaya, N.K.E.M., Mohamed Yusoff, M.A., Hashim, N.H.F., and Abdullah, N.S., 2021, Adsorption of methylene blue from aqueous solution by peanut shell based activated carbon, *Mater. Today: Proc.*, 47, 1246–1251.

[52] Zhang, W., Wang, Y., Fan, L., Liu, X., Cao, W., Ai, H., Wang, Z., Liu, X., and Jia, H., 2022, Sorbent properties of orange peel-based biochar for different pollutants in water, *Processes*, 10 (5), 856.

[53] Zhang, W., Liu, M., Zhao, Y., and Liao, Q., 2022, Facile preparation of porous carbon derived from pomelo peel for efficient adsorption of methylene blue, *Molecules*, 27 (10), 3096.

[54] Dong, P., Liu, H., Xu, S., Chen, C., Feng, S., and Long, A., 2021, Sheet-like skeleton carbon derived from shaddock peels with hierarchically porous structures for ultra-fast removal of methylene blue, *Water*, 13 (18), 2554.

[55] Ding, J., Zhong, Q., and Zhang, S., 2014, Catalytic efficiency of iron oxides in decomposition of H_2O_2 for simultaneous NO_X and SO_2 removal: Effect of calcination temperature, *J. Mol. Catal. A: Chem.*, 393, 222–231.

[56] Ramutshatsha-Makhwedzha, D., Mavhungu, A., Moropeng, M.L., and Mbaya, R., 2022, Activated carbon derived from waste orange and lemon peels for the adsorption of methyl orange and methylene blue dyes from wastewater, *Heliyon*, 8 (8), e09930.

[57] Zhu, S., Xu, J., Kuang, Y., Cheng, Z., Wu, Q., Xie, J., Wang, B., Gao, W., Zeng, J., Li, J., and Chen, K., 2021, Lignin-derived sulfonated porous carbon from cornstalk for efficient and selective removal of cationic dyes, *Ind. Crops Prod.*, 159, 113071.

[58] Donphai, W., Musikanon, N., Du, Z., Sangteantong, P., Chainarong, K., and Chareonpanich, M., 2022, Preparation of C-Zn functionalized MCM-41 from bagasse heavy ash for adsorption of volatile organic compounds, *Mater. Lett.*, 307, 131065.

[59] de Souza, C.C., de Souza, L.Z.M., Yılmaz, M., de Oliveira, M.A., da Silva Bezerra, A.C., da Silva, E.F., Dumont, M.R., and Machado, A.R.T., 2022,

Activated carbon of Coriandrum sativum for adsorption of methylene blue: Equilibrium and kinetic modeling, *Cleaner Mater.*, 3, 100052.

[60] de Souza, C.C., Ciriano, M.R., da Silva, E.F., de Oliveira, M.A., da Silva Bezerra, A.C., Dumont, M.R., da Silva, A.C., and Machado, A.R.T., 2023, Activated carbon obtained from cardboard tube waste of immersion thermocouple and adsorption of methylene blue, *Biomass Convers. Biorefin.*, 13 (4), 3297–3308.

[61] Ren, Y., Chen, F., Pan, K., Zhao, Y., Ma, L., and Wei, S., 2021, Studies on kinetics, isotherms, thermodynamics and adsorption mechanism of methylene blue by N and S Co-doped porous carbon spheres, *Nanomaterials*, 11 (7), 1819.

[62] Tran, T.H., Le, H.H., Pham, T.H., Nguyen, D.T., La, D.D., Chang, S.W., Lee, S.M., Chung, W.J., and Nguyen, D.D., 2021, Comparative study on methylene blue adsorption behavior of coffee husk-derived activated carbon materials prepared using hydrothermal and soaking methods, *J. Environ. Chem. Eng.*, 9 (4), 105362.

[63] Firdaus Mohamad Yusop, M., Aziz, A., and Ahmad, M.A., 2022, Conversion of teak wood waste into microwave-irradiated activated carbon for cationic methylene blue dye removal: Optimization and batch studies, *Arabian J. Chem.*, 15 (9), 104081.

[64] El Nemr, A., Shoaib, A.G.M., El Sikaily, A., Mohamed, A.E.D.A., and Hassan, A.F., 2021, Evaluation of cationic methylene blue dye removal by high surface area mesoporous activated carbon derived from *Ulva lactuca*, *Environ. Processes*, 8 (1), 311–332.

[65] Liang, C., Shi, Q., Feng, J., Yao, J., Huang, H., and Xie, X., 2022, Adsorption behaviors of cationic methylene blue and anionic reactive blue 19 dyes onto nano-carbon adsorbent carbonized from small precursors, *Nanomaterials*, 12 (11), 1814.

[66] Bello, R., Rodríguez-Aguado, E., Smith, V.A., Grachev, D., Castellón, E.R., and Bashkova, S., 2022, Ni-doped ordered nanoporous carbon prepared from chestnut wood tannins for the removal and photocatalytic degradation of methylene blue, *Nanomaterials*, 12 (10), 1625.

[67] Que, A., Zhu, T., and Zheng, Y., 2021, Highly efficient removal of methylene blue via hollow graphene-based magnesium silicate, *J. Mater. Sci.*, 56 (29), 16351–16361.

[68] Castro-Muñiz, A., Martínez-Alonso, A., and Tascón, J.M.D., 2009, Effect of PPTA pre-impregnation with phosphoric acid on the porous texture of carbons prepared by CO_2 activation of PPTA chars, *Microporous Mesoporous Mater.*, 119 (1-3), 284–289.

[69] Zhuang, Q.Q., Cao, J.P., Wu, Y., Zhao, M., Zhao, X.Y., Zhao, Y.P., and Bai, H.C., 2021, Heteroatom nitrogen and oxygen co-doped three-dimensional honeycomb porous carbons for methylene blue efficient removal, *Appl. Surf. Sci.*, 546, 149139.

[70] Gholizadeh Khasevani, S., Shahsavari, S., and Gholami, M.R., 2021, Green synthesis of ternary carbon dots (CDs)/MIL-88B (Fe)/Bi_2S_3 nanocomposite via MOF templating as a reusable heterogeneous nanocatalyst and nano-photocatalyst, *Mater. Res. Bull.*, 138, 111204.

[71] Wang, X., Huang, F., Yu, M., Zhang, C., Ding, F., Chen, L., and Chen, H., 2021, Multilayer adsorption of organic dyes on coal tar-based porous carbon with ultra-high specific surface area, *Int. J. Environ. Sci. Technol.*, 18 (12), 3871–3882.

[72] Liu, H., Tian, X., Xiang, X., and Chen, S., 2022, Preparation of carboxymethyl cellulose/graphene composite aerogel beads and their adsorption for methylene blue, *Int. J. Biol. Macromol.*, 202, 632–643.

[73] Lian, Y.M., Utetiwabo, W., Zhou, Y., Huang, Z.H., Zhou, L., Faheem, M., Chen, R.J., and Yang, W., 2019, From upcycled waste polyethylene plastic to graphene/mesoporous carbon for high-voltage supercapacitors, *J. Colloid Interface Sci.*, 557, 55–64.

[74] Mahiuddin, M., and Ochiai, B., 2021, Lemon juice assisted green synthesis of reduced graphene oxide and its application for adsorption of methylene blue, *Technologies*, 9 (4), 96.

[75] Giraldo, S., Robles, I., Godínez, L.A., Acelas, N., and Flórez, E., 2021, Experimental and theoretical insights on methylene blue removal from wastewater

using an adsorbent obtained from the residues of the orange industry, *Molecules*, 26 (15), 4555.

[76] Ying, Z., Chen, X., Li, H., Liu, X., Zhang, C., Zhang, J., and Yi, G., 2021, Efficient adsorption of methylene blue by porous biochar derived from soybean dreg using a one-pot synthesis method, *Molecules*, 26 (3), 661.

[77] Aziz, B.K., Shwan, D.M.S., and Kaufhold, S., 2022, Comparative study on the adsorption efficiency of two different local clays for the cationic dye; Application for adsorption of methylene blue from medical laboratories wastewater, *Silicon*, 14 (3), 893–902.

[78] Achari, V.S., Lopez, R.M., Rajalakshmi, A.S., Jayasree, S., Shibin, O.M., John, D., and Sekkar, V., 2021, Microporous carbon with highly dispersed nano-lanthanum oxide (La_2O_3) for enhanced adsorption of methylene blue, *Sep. Purif. Technol.*, 279, 119626.

[79] Țurcanu, A.A., Matei, E., Râpă, M., Predescu, A.M., Berbecaru, A.C., Coman, G., and Predescu, C., 2022, Walnut shell biowaste valorization via HTC process for the removal of some emerging pharmaceutical pollutants from aqueous solutions, *Int. J. Mol. Sci.*, 23 (19), 11095.

[80] Zhang, Y., Wang, R., Qiu, G., Jia, W., Guo, Y., Guo, F., and Wu, J., 2021, Synthesis of porous material from coal gasification fine slag residual carbon and its application in removal of methylene blue, *Molecules*, 26 (20), 6116.

[81] Hassan, A.F., Mustafa, A.A., Esmail, G., and Awad, A.M., 2023, Adsorption and photo-Fenton degradation of methylene blue using nanomagnetite/potassium carrageenan bio-composite beads, *Arabian J. Sci. Eng.*, 48 (1), 353–373.

[82] Cai, Z., Liu, Q., Li, H., Wang, J., Tai, G., Wang, F., Han, J., Zhu, Y., and Wu, G., 2022, Waste-to-resource strategy to fabricate functionalized MOFs composite material based on durian shell biomass carbon fiber and Fe_3O_4 for highly efficient and recyclable dye adsorption, *Int. J. Mol. Sci.*, 23 (11), 5900.

[83] Sapkota, K.P., Islam, M.A., Hanif, M.A., Akter, J., Lee, I., and Hahn, J.R., 2021, Hierarchical nanocauliflower chemical assembly composed of copper oxide and single-walled carbon nanotubes for enhanced photocatalytic dye degradation, *Nanomaterials*, 11 (3), 696.

[84] Abdulkhair, B.Y., and Elamin, M.R., 2022, Low-cost carbon nanoparticles for removing hazardous organic pollutants from water: Complete remediation study and multi-use investigation, *Inorganics*, 10 (9), 136.

[85] Wen, T., Huang, B., and Zhou, L., 2022, Facile fabrication of magnetic poly(vinyl alcohol)/activated carbon composite gel for adsorptive removal of dyes, *J. Compos. Sci.*, 6 (2), 55.

[86] Mallakpour, S., Behranvand, V., and Mallakpour, F., 2021, Adsorptive performance of alginate/carbon nanotube-carbon dot-magnesium fluorohydroxyapatite hydrogel for methylene blue-contaminated water, *J. Environ. Chem. Eng.*, 9 (2), 105170.

[87] Chen, F., Liang, W., Qin, X., Jiang, L., Zhang, Y., Fang, S., and Luo, D., 2021, Preparation and recycled simultaneous adsorption of methylene blue and Cu^{2+} co-pollutants over carbon layer encapsulated Fe_3O_4/graphene oxide nanocomposites rich in amino and thiol groups, *Colloids Surf., A*, 625, 126913.

[88] Hu, M., Deng, W., Hu, M., Chen, G., Zhou, P., Zhou, Y., and Su, Y., 2021, Preparation of binder-less activated char briquettes from pyrolysis of sewage sludge for liquid-phase adsorption of methylene blue, *J. Environ. Manage.*, 299, 113601.

[89] Rahmawati, F., Wahyuningsih, S., and Pamularsih, A.W., 2006, Synthesis of thin film of TiO_2 on graphite substrate by chemical bath deposition, *Indones. J. Chem.*, 6 (2), 121–126.

[90] Ulfa, M., Oktaviani, S.L., Mulyani, B., and Sholeha, N.A., 2025, Metal oxide for fast adsorption system in the methylene blue removal, *Indones. J. Chem.*, 25 (2), 619–637.

[91] Lhimr, S., Bouhlassa, S., and Ammary, B., 2019, Effect of molar ratio on structural and size of ZnO/C nanocomposite synthesized using a colloidal method at low temperature, *Indones. J. Chem.*, 19 (2), 422–429.

[92] Ulfa, M., Trisunaryanti, W., Falah, I.I., and Kartini, I., 2016, Wormhole-like mesoporous carbons from gelatine as multistep infiltration effect, *Indones. J. Chem.*, 16 (3), 239–242.

[93] Ulfa, M., and Apriliani, W., 2023, Comparative study of soft template on gunningite synthesis for ibuprofen adsorption application, *Indones. J. Chem.*, 23 (2), 438–448.

[94] Utubira, Y., Wijaya, K., Triyono, T., and Sugiharto, E., 2006, Preparation and characterization of TiO_2–zeolite and its application to degrade textile wastewater by photocatalytic method, *Indones. J. Chem.*, 6 (3), 231–237.

[95] Ulfa, M., and Purnama Ali, M.A., 2022, Influence of calcination temperatures on gunningite-based gelatin template and its application as ibuprofen adsorption, *Indones. J. Chem.*, 22 (6), 1684–1692.

[96] Trisunaryanti, W., Novianti, S.A., Fatmawati, D.A., Triyono, T., Ulfa, M., and Prasetyoko, D., 2022, Simple and green preparation of ZnO blended with highly magnetic silica sand from Parangtritis Beach as catalyst for oxidative desulfurization of dibenzothiophene, *Indones. J. Chem.*, 22 (2), 455–467.